

# Liquid–Liquid Phase Transition of Protein Aqueous Solutions Isothermally Induced by Protein Cross-Linking

Ying Wang and Onofrio Annunziata\*

Department of Chemistry, Texas Christian University, Fort Worth, Texas 76129

Received October 16, 2007. In Final Form: November 28, 2007

We experimentally demonstrated that liquid–liquid phase separation (LLPS) of protein aqueous solutions can be induced by isothermal protein oligomerization. This phenomenon is analogous to LLPS induced by the polymerization of small organic molecules in solution. Specifically, using glutaraldehyde for protein cross-linking, we observed the formation of protein-rich liquid droplets for bovine serum albumin and chicken egg lysozyme at 25 °C. These droplets evolved into cross-linked protein microspheres. If the aqueous solutions of the protein monomer do not show LLPS at temperatures lower than the oligomerization temperature, protein-rich droplets are not observed. We experimentally linked the formation of these droplets to the increase of LLPS temperature during protein oligomerization. When macroscopic aggregation competes with LLPS, a rationale choice of pH, polyethylene glycol, and salt concentrations can be used to favor LLPS relative to aggregation. Although glutaraldehyde has been extensively used to cross-link protein molecules, to our knowledge, its use in homogeneous aqueous solutions to induce LLPS has not been previously described. This work contributes to the fundamental understanding of both phase transitions of protein solutions and the morphology of protein condensed phases. It also provides guidance for the development of new methods based on mild experimental conditions for the preparation of protein-based materials.

## Introduction

Isothermal polymerization reactions of small organic molecules can bring about phase transitions from initially homogeneous liquid mixtures.<sup>1–7</sup> This phenomenon is quite common in industrial polymerization processes.<sup>8</sup> The observed phase separation is related to the poor monomer–solvent miscibility and to the decrease of solution mixing entropy caused by polymerization. The interplay between polymerization and phase transitions is responsible for various microscopic two-phase patterns. Hence, several types of polymer-rich phases such as crystals, amorphous aggregates, microspheres, or bicontinuous gel-like networks can be produced depending on the chosen experimental conditions. According to the type of application, one polymer-rich phase is preferred with respect to another. Thus, polymerization-induced phase transitions have been extensively studied to understand and control phase morphologies.<sup>1–8</sup>

Polymerization reactions also involve large molecules such as proteins. For example, actin<sup>9</sup> and sickle-cell hemoglobin<sup>10,11</sup> are known to undergo polymerization in living organisms. Hence, protein association in aqueous solutions has been investigated for understanding both the behavior of living systems and the

formation of protein aggregates associated with various diseases.<sup>9–14</sup>

The association of proteins also can be intentionally induced by chemical cross-linking, using bifunctional agents such as glutaraldehyde.<sup>13,15–22</sup> Protein cross-linking has found applications in biochemistry for studying protein–protein interactions<sup>19,20</sup> and crystallography for the chemical stabilization of good-quality protein crystals.<sup>23</sup> Furthermore, since proteins display important chemical properties such as ligand binding, catalytic activity, chemical-environment sensitivity, biocompatibility, molecular recognition, and versatility to chemical modifications, they are very valuable for applications in biotechnology and materials science. Thus, cross-linking is also used for the preparation of protein-based materials.<sup>21,22</sup> For instance, in enzymology, cross-

\* To whom correspondence should be addressed. Tel.: (817) 257-6215; fax: (817) 257-5851; e-mail: O.Annunziata@tcu.edu.

(1) Nephew, J. B.; Nihei, T. C.; Carter, S. A. *Phys. Rev. Lett.* **1998**, *80*, 3276–3279.

(2) Tran-Cong, Q.; Harada, A. *Phys. Rev. Lett.* **1996**, *76*, 1162–1165.

(3) Kyu, T.; Lee, J. H. *Phys. Rev. Lett.* **1996**, *76*, 3746–3749.

(4) Williams, R. J. J.; Rozenberg, B. A.; Pascault, J. P. *Adv. Polym. Sci.* **1997**, *128*, 95–156.

(5) Luo, K. *Eur. Polym. J.* **2006**, *42*, 1499–1505.

(6) Wang, X.; Okada, M.; Matsushita, Y.; Furukawa, H.; Han, C. C. *Macromolecules* **2005**, *38*, 7127–7133.

(7) Kimura, K.; Kohama, S.-I.; Yamazaki, S. *Polym. J.* **2006**, *38*, 1005–1022.

(8) Sperling, L. H. *Polymeric Multicomponent Materials: An Introduction*; John Wiley and Sons: New York, 1997.

(9) Oosawa, F.; Asakura, S. *Thermodynamics of the Polymerization of Protein*; Academic Press: New York, 1975.

(10) Aprelev, A.; Weng, W. J.; Zakharov, M.; Rotter, M.; Yosmanovich, D.; Kwong, S.; Briehl, R. W.; Ferrone, F. A. *J. Mol. Biol.* **2007**, *369*, 1170–1174.

(11) Galkin, O.; Nagel, R. L.; Vekilov, P. G. *J. Mol. Biol.* **2007**, *365*, 425–439.

(12) Stradner, A.; Sedgwick, H.; Cardinaux, F.; Poon, W. C. K.; Egelhaaf, S. U.; Schurtenberger, P. *Nature (London, U.K.)* **2004**, *432*, 492–495.

(13) Bitan, G.; Kirkitadze, M. D.; Lomakin, A.; Vollers, S. S.; Benedek, G. B.; Teplow, D. B. *Proc. Natl. Acad. Sci. U.S.A.* **2003**, *100*, 330–335.

(14) Annunziata, O.; Pande, A.; Pande, J.; Ogun, O.; Lubsen, N. H.; Benedek, G. B. *Biochemistry* **2005**, *44*, 1316–1328.

(15) Margolin, A. L.; Navia, M. A. *Angew. Chem., Int. Ed.* **2001**, *40*, 2204–2222.

(16) Abraham, T. E.; Roy, J. J. *J. Chem. Rev.* **2004**, *104*, 3705–3721.

(17) Schoevaart, R.; Wolbers, M. W.; Golubovic, M.; Ottens, M.; Kieboom, A. P. G.; van Rantwijk, F.; van der Wielen, L. A. M.; Sheldon, R. A. *Biotechnol. Bioeng.* **2004**, *87*, 754–762.

(18) Langer, K.; Balthasar, S.; Vogel, V.; Dinauer, N.; von Briesen, H.; Schubert, D. *Int. J. Pharm.* **2003**, *257*, 169–180.

(19) Wong, S. S. *Chemistry of Protein Conjugation and Cross-Linking*; CRC Press: Boca Raton, FL, 1993.

(20) Kluger, R.; Alagic, A. *Bioorg. Chem.* **2004**, *32*, 451–472.

(21) De Wolf, F. A.; Brett, G. M. *Pharmacol. Rev.* **2000**, *52*, 207–236.

(22) Ayala, M.; Vasquez-Duhalt, R. *Enzymatic Catalysis on Petroleum Products, in Studies in Surface Science and Catalysis, Vol. 151*; Vasquez-Duhalt, R., Quintero-Ramirez, R., Eds.; Elsevier: Amsterdam, 2004; pp 67–111.

(23) McPherson, A. *Crystallization of Biological Macromolecules*; Cold Spring Harbor Press: New York, 1998.

(24) Anderson, V. J.; Lekkerkerker, H. N. W. *Nature (London, U.K.)* **2002**, *416*, 811–815.

(25) ten Wolde, P. R.; Frenkel, D. *Science (Washington, DC, U.S.)* **1997**, *277*, 1975–1978.

(26) Broide, M. L.; Berland, C. R.; Pande, J.; Ogun, O.; Benedek, G. B. *Proc. Natl. Acad. Sci. U.S.A.* **1991**, *88*, 5660–5664.

(27) Asherie, N.; Lomakin, A.; Benedek, G. B. *Phys. Rev. Lett.* **1996**, *77*, 4832–4835.

linked enzyme crystals and aggregates find applications relevant to petroleum products, due to their superior stability and recyclability as compared to the free enzyme.<sup>15–17,22</sup> In pharmaceuticals, cross-linked albumin microspheres are used for loading drugs relevant to medical diagnosis and drug delivery.<sup>18</sup> These applications of proteins as materials are expected to steadily increase due to protein engineering.<sup>22</sup>

In the absence of cross-linking agents, protein aqueous solutions are generally subject to phase transformations such as crystallization, aggregation, and gelation, depending on the experimental conditions.<sup>23,28–42</sup> Currently, it is not well-understood as to how a given experimental condition favors one transformation relative to another. Moreover, few protein–buffer systems (i.e., lysozyme and several eye-lens proteins) are known to undergo liquid–liquid phase separation (LLPS) by lowering the temperature of homogeneous protein solutions.<sup>26,34,36</sup> This phase transition can be observed for a wider range of protein cases if polyethylene glycol (PEG) is added to the protein–buffer systems.<sup>38,40</sup> Since LLPS is driven by the presence of net attractive interactions between protein molecules,<sup>41</sup> the location of the corresponding phase boundary in the temperature–concentration phase diagram has been measured to characterize molecular interactions.<sup>26,27,37–42</sup> Furthermore, LLPS is metastable with respect to other phase transformations.<sup>27</sup> Thus, this phase transition is interesting not only because it competes with crystallization, aggregation, and gelation but also because it provides a distinctive kinetic route for these other processes.<sup>24,25,32,34</sup> Finally, the phase behavior of protein solutions becomes even more intriguing if proteins undergo chemical association in solution.<sup>14</sup>

Here, we demonstrate that, under specific experimental conditions, the addition of glutaraldehyde to homogeneous aqueous solutions can isothermally induce LLPS and the consequent formation of cross-linked protein-rich droplets. We relate this phenomenon to protein oligomerization in solution. This behavior is analogous to the phase separation induced by the polymerization of small organic molecules. Although glutaraldehyde has been extensively used to cross-link protein molecules,<sup>15–19</sup> to our knowledge, its use in homogeneous solutions to induce LLPS has not been previously described. Understanding as to how protein cross-linking induces LLPS and the design of the experimental conditions that favors this process is of fundamental importance for applications of proteins in chemistry, biology, and materials science.

## Materials and Methods

**Materials.** Bovine serum albumin and chicken egg lysozyme were purchased from Sigma. The molecular weight was assumed to be 66.4 kg/mol for serum albumin and 14.3 kg/mol for lysozyme. HPLC (System Gold, Beckman Coulter) with a size-exclusion column (Biosep-SEC-S 2000, Phenomenex) on lysozyme showed the purity to be better than 99%. In the case of serum albumin, HPLC shows the presence of 20% oligomers. Thus, further purification was performed for albumin using size-exclusion preparative chromatography.<sup>40</sup> The column was packed using Sephacryl S-200 purchased from GE Healthcare. The mobile phase was a sodium phosphate buffer (0.05 M, pH 7.1), and the flow rate was 1.5 mL/min. The serum albumin monomer fraction was collected and stored at 4 °C. Size-exclusion HPLC on the monomer fraction showed the purity to be better than 99%. Protein solutions were then dialyzed exhaustively (Amicon, Millipore) into the desired aqueous buffer. The concentration of serum albumin in solution was determined by UV absorption at 278 nm (DU 800 spectrophotometer, Beckman Coulter), using an extinction coefficient value of 0.667 mg<sup>-1</sup> mL cm<sup>-1</sup>.<sup>43</sup> The concentration of lysozyme in solution was determined by UV absorption at 280 nm, using an extinction coefficient value of 2.64 mg<sup>-1</sup> mL cm<sup>-1</sup>.<sup>44</sup> Polyethylene glycol (PEG) with an average molecular weight of 8.0 kg/mol (PEG8000), sodium chloride, and buffer components (sodium acetate, monobasic sodium phosphate, anhydrous dibasic sodium phosphate, and boric acid) were purchased from Fischer Scientific and used without further purification. PEG8000–buffer and NaCl–buffer stock solutions were prepared by weight. Small amounts of these solutions were added to protein–buffer solutions, and the final concentrations were determined by weight. Glutaraldehyde (25% aqueous solution) was purchased from Acros and used without further purification. Glutaraldehyde–buffer stock solutions were prepared by weight. Small aliquots of glutaraldehyde stock solutions were added prior to the physicochemical characterization. Phase separation was complete after a given time that increased as the glutaraldehyde concentration decreased. The final protein concentration in the protein dilute phase (supernatant) was measured and found to decrease as the concentration of glutaraldehyde increased. Within our experimental domain, this concentration ranged from 5 to 90% of the initial protein concentration.

**Microscopy.** After phase separation was completed, the protein condensed phase was observed under a light microscope (Axioskop 40, Zeiss) using phase-contrast microscopy. Images were taken using a digital camera (AxioCam MRC, Zeiss) interfaced by a computer with software (Axiovision AC 4.5, Zeiss). The microsphere size was determined using the ImageJ software. Images were also taken using the more invasive scanning electron microscopy (JSM-6100, JEO). These images confirmed our observations by light microscopy. Energy dispersive X-ray spectroscopy (500, IXRF Systems) shows a significant presence of sulfur inside the microspheres, thereby confirming their high protein concentration.

**Measurements of LLPS Temperature.** The LLPS temperature,  $T_{ph}^0$ , of the cross-linker-free protein aqueous samples was determined by measuring sample turbidity as a function of temperature. A turbidity meter was built by using a programmable circulating bath (1197P, VWR) connected to a homemade optical cell where the sample is located. The temperature at the sample location was measured by using a calibrated thermocouple ( $\pm 0.1$  °C). Light coming from a solid-state laser (633 nm, 5 mW, Coherent) passes through the sample with optical path  $L$  of 0.40 cm, and the transmitted intensity,  $I$ , is measured using a photodiode detector and a computer-interfaced optical meter (1835-C, Newport). For a given transparent sample, the transmitted intensity,  $I_0$ , was measured. The temperature of the water bath was slowly decreased (0.5 °C/min), and the temperature  $T_{ph}^0$  at which the turbidity  $\tau = (1/L) \log(I_0/I)$  shows a sharp increase was taken.<sup>14,40,45</sup> For LLPS measurements during protein cross-linking at 25.0 °C, we determined the LLPS temperature,

(28) Ducruix, A.; Giege, R. *Crystallization of Nucleic Acids and Proteins: A Practical Approach (Practical Approach Series)*; Oxford University Press: Oxford, 1999.

(29) Finet, S.; Vivares, D.; Bonnet, F.; Tardieu, A. *Methods Enzymol.* **2003**, *368*, 105–129.

(30) Chayen, N. E. *Curr. Opin. Struct. Biol.* **2004**, *14*, 577–583.

(31) Yau, S. T.; Vekilov, P. G. *Nature (London, U.K.)* **2000**, *406*, 494–497.

(32) Galkin, O.; Vekilov, P. G. *Proc. Natl. Acad. Sci. U.S.A.* **2000**, *97*, 6277–6281.

(33) Gliko, O.; Neumaier, N.; Pan, W.; Haase, I.; Fischer, M.; Bacher, A.; Weinkauff, S.; Vekilov, P. G. *J. Am. Chem. Soc.* **2005**, *127*, 3433–3438.

(34) Muschol, M.; Rosenberger, F. *J. Chem. Phys.* **1997**, *107*, 1953–1962.

(35) Tanaka, H.; Nishikawa, Y. *Phys. Rev. Lett.* **2005**, *95*, 78103.

(36) Taratuta, V. G.; Holschbach, A.; Thurston, G. M.; Blankschtein, D.; Benedek, G. B. *J. Phys. Chem.* **1990**, *94*, 2140–2144.

(37) Annunziata, O.; Asherie, N.; Lomakin, A.; Pande, J.; Ogun, O.; Benedek, G. B. *Proc. Natl. Acad. Sci. U.S.A.* **2002**, *99*, 14165–14170.

(38) Annunziata, O. J.; Ogun, O.; Benedek, G. B. *Proc. Natl. Acad. Sci. U.S.A.* **2003**, *100*, 970–974.

(39) Bloustone, J.; Virmani, T.; Thurston, G. M.; Fraden, S. *Phys. Rev. Lett.* **2006**, *96*, 87803.

(40) Wang, Y.; Annunziata, O. *J. Phys. Chem. B* **2007**, *111*, 1222–1230.

(41) Lomakin, A.; Asherie, N.; Benedek, G. B. *J. Chem. Phys.* **1996**, *104*, 1646–1656.

(42) Petsev, D. N.; Wu, X. X.; Galkin, O.; Vekilov, P. G. *J. Phys. Chem. B* **2003**, *107*, 3921–3926.

(43) Foster, J. F.; Serman, M. D. *J. Am. Chem. Soc.* **1956**, *78*, 3656–3660.

(44) Sophianopoulos, A. J.; Rhodes, C. K.; Holcomb, D. N.; van Holde, K. E. *J. Biol. Chem.* **1962**, *237*, 1107–1112.

$T_{\text{ph}}$ , as a function of time from the beginning of cross-linking. For these experiments, a given aliquot of the reacting mixture was transferred into a test tube, and its temperature promptly decreased, to minimize the measurement time. The time and temperature at which the sample turbidity shows a sharp increase were taken.

**Measurements of Turbidity Induction Times.** After glutaraldehyde was added to the protein samples, the turbidity was monitored as a function of time at  $25.0 \pm 0.1$  °C. For the oligomerization-induced LLPS experiments, the value of  $\tau(t)$  remained equal to zero after the addition of glutaraldehyde. However, after a well-defined and reproducible induction time was reached, a rapid increase of turbidity was observed. To characterize the rate of opacification, we determined the induction time,  $t_{\text{ind}}$ , by extrapolation of the turbidity data to zero turbidity.

**Measurements of Light Scattering.** Measurements of static and dynamic light scattering were performed at  $25.0 \pm 0.1$  °C. After glutaraldehyde was added, all protein samples were promptly filtered through a  $0.02 \mu\text{m}$  filter (Anotop 10, Whatman) and placed in a test tube. The experiments were performed on a light-scattering apparatus built using the following main components: He–Ne laser (35 mW, 632.8 nm, Coherent Radiation), manual goniometer and thermostat (Photocor Instruments), multi-tau correlator, and APD detector and software (PD4042, Precision Detectors). All measurements were performed at a scattering angle of 90°. The protein contribution to light-scattering intensity,  $i_s$ , was obtained by removing the scattered intensity contributions of the corresponding protein-free samples. The scattered intensity ratio  $i_s/i_s^0$ , where  $i_s^0$  is the initial value of  $i_s$ , was then calculated. The dynamic light scattering (DLS) correlation functions were analyzed using a regularization algorithm (Precision Deconvolve 32, Precision Detectors).<sup>46</sup> For monomodal distributions, the apparent hydrodynamic radius,  $R_h$ , was calculated using the Stokes–Einstein equation:  $R_h = k_B T / (6\pi\eta\langle D \rangle_z)$ ,<sup>47</sup> where  $k_B$  is the Boltzmann constant,  $T$  is the absolute temperature,  $\eta$  is the viscosity of the protein-free mixtures, and  $\langle D \rangle_z$  is the  $z$ -average diffusion coefficient. After a given induction time, a second light-scattering peak corresponding to protein clusters was observed. The hydrodynamic radius,  $R_h^{(c)}$ , was calculated from the  $z$ -average diffusion coefficient of this slow diffusion mode.

## Results and Discussion

**Oligomerization-Induced LLPS of Albumin Solutions.** We performed protein cross-linking reactions in aqueous solutions of bovine serum albumin using glutaraldehyde as the cross-linking agent. Although the mechanism of protein–glutaraldehyde binding is rather complex due to the participation of glutaraldehyde oligomers, it is well-established that this bifunctional cross-linker mainly reacts with the  $\epsilon$ -amino group of the lysines located on the protein surface. Cross-linking experiments were performed as a function of glutaraldehyde concentration at a protein concentration of 10 mg/mL and at pH 5.2, close to the isoelectric point.<sup>48</sup>

At pH 5.2, we previously reported LLPS of albumin aqueous solutions. We found that LLPS of albumin–buffer solutions does not occur for protein concentrations as high as 400 mg/mL and temperatures as low as  $-15$  °C. However, if PEG is added to the albumin–buffer solutions, LLPS can be readily induced by lowering the sample temperature. The effect of PEG can be described through the influence of mutual volume exclusion on the entropy of the system, thereby creating an effective attraction between the protein molecules responsible for LLPS.<sup>49,50</sup> This mechanism is usually denoted using the terms: depletion

interactions<sup>51</sup> or macromolecular crowding.<sup>52</sup> Models based on this mechanism have been qualitatively successful in describing the effect of PEG on the LLPS of protein solutions for several protein cases including albumin.<sup>37,38,40</sup>

We performed albumin cross-linking in the presence and absence of PEG at 25 °C. Our main results are summarized in Figure 1a–c for the cross-linking experiments in the presence of PEG (PEG8000 6.0% (w/w)) and in Figure 1d for those in the absence of PEG. Figure 1a–c illustrates the presence of protein-rich droplets typical of LLPS at three cross-linker concentrations. The LLPS boundary of the corresponding cross-linker-free system is located at  $T_{\text{ph}}^0 = -12$  °C. As we will discuss later in more detail, protein oligomerization is responsible for increasing the LLPS temperature, thereby bringing the system into a nonequilibrium state at the reaction temperature (25 °C). Contrary to ordinary LLPS, this process is irreversible due to chemical cross-linking. Hence, the final product is cross-linked protein microspheres. For the experiments in the absence of PEG, protein aggregates with no defined morphology were observed by both light microscopy and scanning electron microscopy. These amorphous aggregates are shown in Figure 1d. Thus, our results demonstrate that the presence of the LLPS boundary in the phase diagram of protein solutions qualitatively affects the morphology of the protein condensed phase generated from cross-linking.

From Figure 1a–c, we can also observe that the average radius of the final cross-linked microspheres decreases as the glutaraldehyde concentration increases. To explicitly show this behavior, we report the average radius,  $R$ , of the microspheres as a function of cross-linker concentration in Figure 2a. Correspondingly, in Figure 2b, we show that  $R^{-1}$  linearly decreases with  $c_{\text{CL}}$ , approaching zero as the cross-linker concentration vanishes. The observed behavior suggests that the final size of the microspheres is governed by the nucleation of the protein-rich droplets from the metastable solution. According to nucleation theory,<sup>53</sup> the radius of the critical nucleus decreases as the supersaturation increases. Thus, if a higher cross-linker concentration brings the system into a higher final supersaturation with respect to LLPS, the average radius of the nucleating particles decreases as the cross-linker concentration increases.

**Oligomerization-Induced LLPS of Lysozyme Solutions.** We also performed protein cross-linking reactions in aqueous solutions of chicken egg-white lysozyme at 25 °C using glutaraldehyde as the cross-linking agent. Cross-linking experiments were performed as a function of glutaraldehyde concentration at a protein concentration of 10 mg/mL.

Lysozyme is known to undergo LLPS without the assistance of PEG. LLPS in lysozyme aqueous solutions has been previously reported at pH 4.5 and 7.1. Consequently, we performed our cross-linking experiments at these experimental conditions. We observed that lysozyme has a net positive charge at these two pH values ( $\text{pI} \approx 11$ ).<sup>54</sup> This implies that salt must be added to the protein solutions to screen electrostatic repulsive interactions between the protein molecules. For all our lysozyme experiments, we experimentally measured the LLPS temperature,  $T_{\text{ph}}^0$ , of the corresponding cross-linker-free systems.

(49) Tardieu, A.; Bonnete, F.; Finet, S.; Vivares, D. *Acta Crystallogr., Sect. D: Biol. Crystallogr.* **2002**, *58*, 1549–1553.

(50) Adams, M.; Fraden, S. *Biophys. J.* **1998**, *74*, 669–677.

(51) Kulkarni, A. M.; Chatterjee, A. P.; Schweizer, K. S.; Zukoski, C. F. *Phys. Rev. Lett.* **1999**, *83*, 4554–4557.

(52) Hall, D.; Minton, A. P. *Biochim. Biophys. Acta* **2003**, *1649*, 127–139.

(53) Kashchiev, D. *Nucleation: Basic Theory with Applications*; Butterworth–Heinemann: Oxford, 2000.

(54) Tanford, C.; Wagner, M. L. *J. Am. Chem. Soc.* **1954**, *76*, 3331–3336.

(45) Liu, C.; Asherie, N.; Lomakin, A.; Pande, J.; Ogun, O.; Benedek, G. B. *Proc. Natl. Acad. Sci. U.S.A.* **1996**, *93*, 377–382.

(46) Lomakin, A.; Teplow, D. B.; Benedek, G. B. *Methods Mol. Biol.* **2005**, *299*, 153–174.

(47) Pecora, R. *Dynamic Light Scattering*; Plenum Press: New York, 1985.

(48) Tanford, C.; Swanson, S. A.; Shore, S. A. *J. Am. Chem. Soc.* **1955**, *77*, 6414–6421.

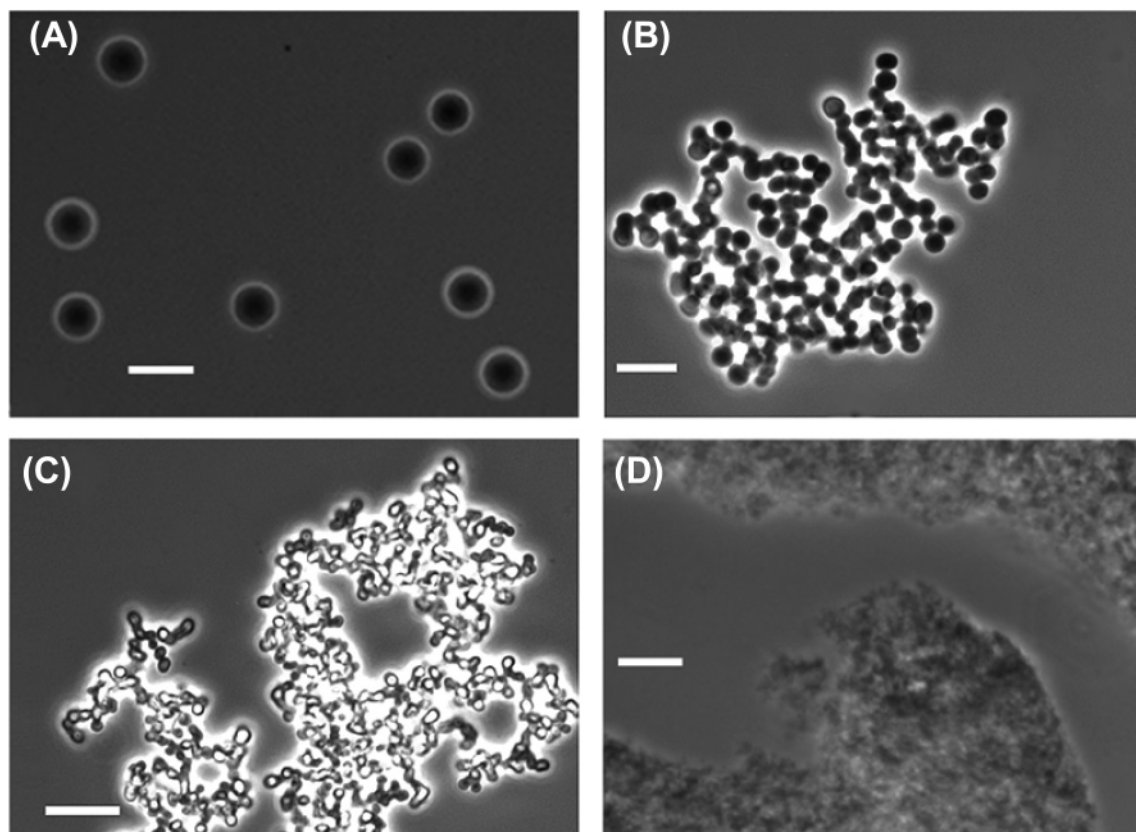


**Figure 1.** Images taken with a light microscope using phase contrast. LLPS induced by albumin cross-linking at 25 °C and at three representative glutaraldehyde concentrations: (A)  $c_{CL} = 0.075\%$ ; (B)  $c_{CL} = 0.15\%$ ; and (C)  $c_{CL} = 0.30\%$ . The cross-linked microspheres were obtained from 10 mg/mL albumin in aqueous sodium acetate buffer, 0.1 M, pH 5.2, PEG8000 6.0% (w/w) at 25 °C. The LLPS temperature of the cross-linker-free system is  $T_{ph}^0 = -12$  °C. (D) Cross-linked amorphous aggregates obtained from 10 mg/mL albumin in aqueous sodium acetate buffer, 0.1 M, pH 5.2,  $c_{CL} = 0.1\%$  at 25 °C. The length of the horizontal bars is 10  $\mu\text{m}$ .

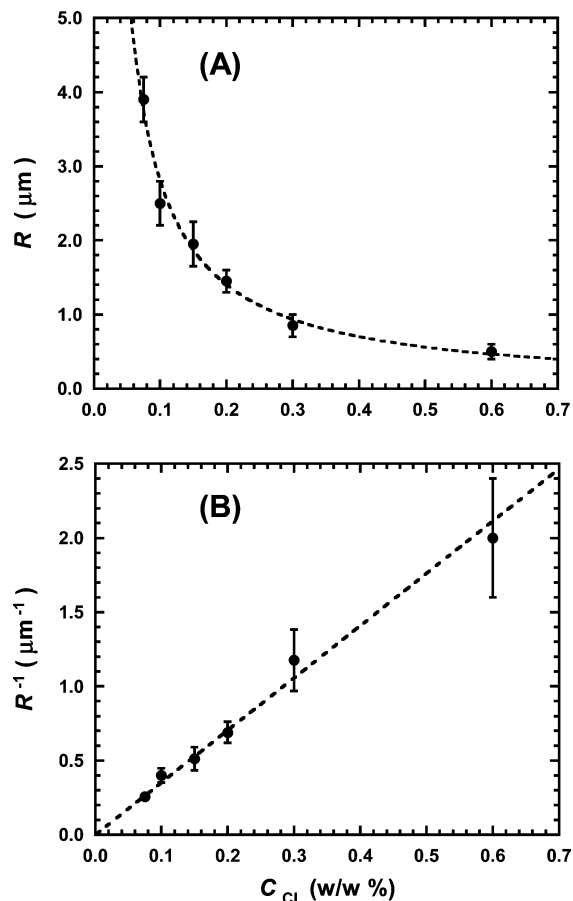
Our results are summarized in Figure 3a,b. Figure 3 illustrates the presence of protein-rich droplets for lysozyme at pH 4.5 and 7.1. We found that the phase-separation process of albumin solutions at pH 5.2 is significantly faster than that of lysozyme solutions at pH 4.5–7.1. This can be related to the significantly lower number of lysines of lysozyme (six) as compared to albumin (60). Moreover, contrary to the albumin case, the size of the cross-linked protein microspheres was found to be independent of the cross-linker concentration. This suggests that the final size of the microspheres does not decrease as the rate of nucleation increases. In this case, the growth rate of the droplets may also play a significant role.

Since the phase-separation process of the lysozyme solutions is relatively slow, we accurately examined the effect of pH and NaCl concentration on the kinetics of LLPS separation by determining the turbidity of the protein samples as a function of time from the beginning of the reaction. As shown in Figure 4a, the turbidity is observed to sharply increase after a well-defined and reproducible induction time,  $t_{ind}$ , which can be used to characterize the rate of phase separation. In Figure 4b, we show that  $t_{ind}^{-1}$  increases with the cross-linker concentration,  $c_{CL}$ , as expected. At a given pH and cross-linker concentration,  $t_{ind}^{-1}$  increases with salt concentration. This effect, which is larger at pH 4.5 than at pH 7.1, can be related to the corresponding effect of the salt concentration on  $T_{ph}^0$  because a higher value of  $T_{ph}^0$  implies a smaller difference between the initial LLPS temperature and the cross-linking temperature. Moreover, an increase in  $T_{ph}^0$  is also related to a corresponding increase in the magnitude of protein–protein attractive interactions. This favors cross-linking by promoting more contacts between the protein molecules. Finally, Figure 4b also shows that  $t_{ind}^{-1}$  significantly

increases with the pH at a given cross-linker concentration. This effect is mainly related to the corresponding increase in chemical reactivity of the lysine  $\epsilon$ -amino groups of the protein.<sup>19</sup> Indeed, the  $t_{ind}^{-1}$  values at pH 7.1 are significantly higher than those at pH 4.5 even when  $T_{ph}^0$  at pH 4.5 is higher than at pH 7.1.

To further characterize the effect of pH on phase separation, we also performed cross-linking of the lysozyme at pH 9.1 closer to the isoelectric point. At this pH, measurements of static and dynamic light scattering show that the lysozyme undergoes aggregation even in the absence of cross-linkers. Interestingly, the aggregation rate decreases as the NaCl concentration increases. This behavior can be related to the weakening effect of salts on electrostatic attractive interactions between the oppositely charged surface groups of the protein molecules. However, we remark that the LLPS temperature increases with the NaCl concentration. This implies that salt favors LLPS with respect to aggregation. We also investigated protein aggregation in the presence of PEG. We found that both aggregation rate and LLPS temperature increase with the PEG concentration. This behavior is consistent with the presence of depletion forces, which enhance protein–protein attraction, thereby favoring both aggregation and LLPS.

The effect of cross-linking on the phase separation of lysozyme solutions is consistent with the observed behavior. In the presence of NaCl at 0.5 M and higher concentrations, we observed the formation of droplets (see Figure 5a). On the other hand, at low salt concentrations or in the presence of PEG, we observed the formation of amorphous macroscopic aggregation (see Figure 5b). For the latter case, the corresponding sample turbidity steadily increases with time, contrary to the typical turbidity profile associated with oligomerization-induced LLPS. Hence, the presence of the LLPS boundary in the protein–solution phase



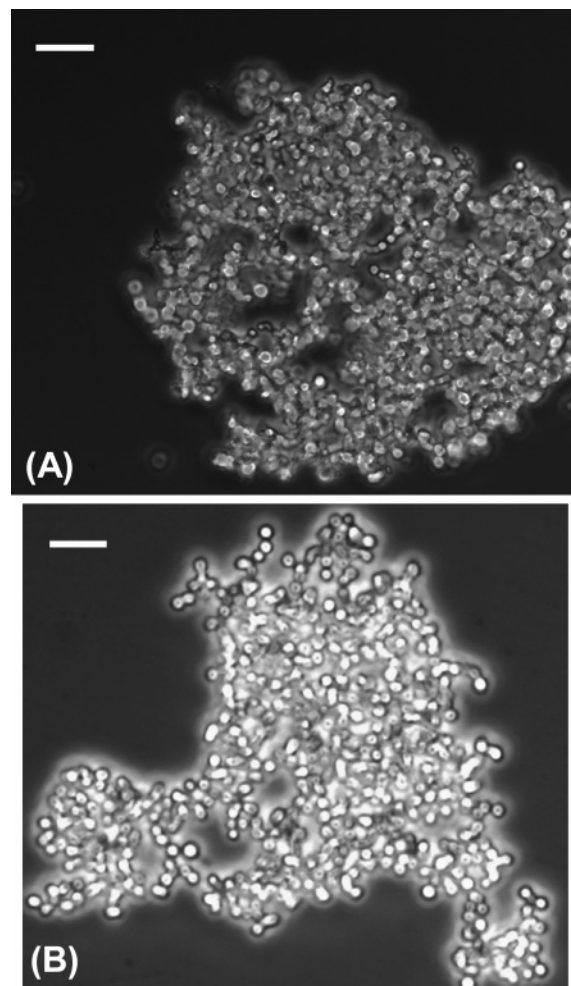
**Figure 2.** (A) Average radius of albumin microspheres,  $R$ , as a function of glutaraldehyde concentration,  $c_{\text{CL}}$ . The experimental conditions are those described for Figure 1. (B) Inverse of  $R$  as a function of  $c_{\text{CL}}$ . The  $R^{-1}$  data were fitted to straight lines.

diagram may not necessarily lead to the formation of protein-rich droplets if protein aggregation is relatively fast. From these observations, we deduced that specific conditions of pH, PEG, and salt concentrations can be chosen so that LLPS is favored with respect to aggregation.

In the following two sections, we will examine two important aspects of oligomerization-induced LLPS in more detail: (1) the effect of oligomerization on the LLPS temperature and (2) the kinetic evolution of oligomerization-induced LLPS. We will focus on the following two systems: albumin-PEG8000-buffer at pH 5.2 and lysozyme-NaCl-buffer at pH 4.5. For the lysozyme system, we successfully used DLS to monitor the onset of phase separation since the corresponding cross-linking rate was sufficiently slow.

**Effect of Oligomerization on LLPS Temperature.** As the degree of oligomerization increases, the LLPS boundary moves toward higher temperatures. To experimentally demonstrate this effect, we performed measurements of the LLPS temperature,  $T_{\text{ph}}$ , as a function of time,  $t$ , starting from the initial LLPS temperature,  $T_{\text{ph}}^0$ , of the protein monomer. In Figure 6a, we experimentally demonstrate the increase of  $T_{\text{ph}}$  with time for both protein cases. As expected, the rate of increase of the LLPS temperature found for albumin was significantly larger than that found for lysozyme.

To further examine the effect of oligomerization on the LLPS temperature, we measured the protein contribution to light-scattering intensity,  $i_s$ , as a function of time starting from the initial intensity,  $i_s^0$ . In Figure 6b, we report the absolute temperature ratio:  $T_{\text{ph}}/T_{\text{ph}}^0$  as a function of the corresponding



**Figure 3.** Images taken with a light microscope using phase contrast. LLPS induced by lysozyme cross-linking at 25 °C. Cross-linked lysozyme microspheres are reported for two representative cases: (A) 10 mg/mL lysozyme in aqueous sodium acetate buffer, 0.1 M, pH 4.5, NaCl 0.5 M,  $c_{\text{CL}} = 0.1\%$ ,  $T_{\text{ph}}^0 = -12$  °C and (B) 10 mg/mL lysozyme in sodium phosphate buffer, 0.1 M, pH 7.1, NaCl 1.0 M,  $c_{\text{CL}} = 0.1\%$ ,  $T_{\text{ph}}^0 = -1.7$  °C. The length of the horizontal bars is 10  $\mu\text{m}$ .

intensity ratio  $i_s/i_s^0$ . Since the light-scattering intensity is directly proportional to the mass-average molecular weight of the protein oligomers, the ratio  $i_s/i_s^0$  is equal to the mass-average degree of oligomerization.<sup>55</sup> We can see that the  $T_{\text{ph}}/T_{\text{ph}}^0$  curves reported as a function of  $i_s/i_s^0$  in Figure 6b are close to each other, even though the  $T_{\text{ph}}$  curves in Figure 6a are significantly separated. Thus, the effect of oligomerization on the LLPS temperature is similar for both proteins.

The increase of  $T_{\text{ph}}$  with the degree of polymerization has been theoretically investigated.<sup>56–60</sup> Since models based on hard spheres have been used to describe the phase behavior of protein solutions,<sup>41</sup> those based on hard-sphere chains<sup>57–60</sup> will be used to examine the effect of protein oligomerization. Banaszak et al.<sup>57</sup> have reported a perturbation theory based on Wertheim's theoretical framework<sup>60</sup> to determine the effect of hard-sphere

(55) Munk, P.; Aminabhavi, T. M. *Introduction to Macromolecular Science*, 2nd ed.; John Wiley and Sons: New York, 2002.

(56) Kindt, J. T.; Gelbart, W. M. *J. Chem. Phys.* **2001**, *114*, 1432–1439.

(57) Banaszak, M.; Chiew, Y. C.; Radosz, M. *Phys. Rev. E: Stat., Nonlinear, Soft Matter Phys.* **1993**, *48*, 3760–3765.

(58) Yethiraj, A.; Hall, C. K. *J. Chem. Phys.* **1991**, *95*, 8494–8506.

(59) Chapman, W. G.; Gubbins, K. E.; Jackson, G.; Radosz, M. *Ind. Eng. Chem. Res.* **1990**, *29*, 1709–1717.

(60) Wertheim, M. S. *J. Chem. Phys.* **1986**, *85*, 2929–2936.

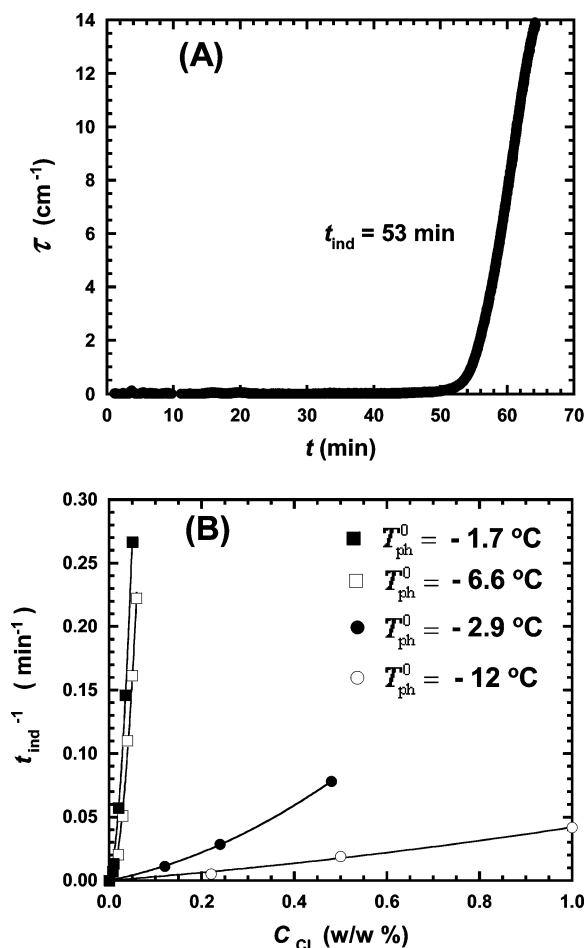


**Figure 4.** (A) Turbidity,  $\tau$ , as a function of time,  $t$ , after cross-linking has started. This turbidity profile was obtained at 25 °C for the representative case: 10 mg/mL lysozyme in aqueous sodium acetate buffer, 0.1 M, pH 4.5, NaCl 0.5 M,  $c_{\text{CL}} = 0.5\%$ . (B) Inverse of the induction time,  $t_{\text{ind}}$ , as a function of  $c_{\text{CL}}$  for four representative cases at 25 °C: 10 mg/mL lysozyme in aqueous sodium acetate buffer, 0.1 M, pH 4.5, NaCl 0.5 M,  $T_{\text{ph}}^0 = -12$  °C (open circles); 10 mg/mL lysozyme in aqueous sodium acetate buffer, 0.1 M, pH 4.5, NaCl 1.0 M,  $T_{\text{ph}}^0 = -2.9$  °C (closed circles); 10 mg/mL lysozyme in aqueous sodium phosphate buffer, 0.1 M, pH 7.1, NaCl 0.5 M,  $T_{\text{ph}}^0 = -6.6$  °C (open squares); and 10 mg/mL lysozyme aqueous sodium phosphate buffer, 0.1 M, pH 7.1, NaCl 1.0 M,  $T_{\text{ph}}^0 = -1.7$  °C (closed squares). The solid curves are guides for the eye.

connectivity on the LLPS phase boundary. This theory was found to be in good agreement with the Monte Carlo results of Yethiraj and Hall.<sup>58</sup> In their model, chain connectivity is introduced by applying thermodynamic perturbation theory to the hard-sphere monomer<sup>59</sup> with diameter  $\sigma$ . The chain–chain attractive interactions, which are responsible for LLPS, were introduced using the square-well potential<sup>61</sup> for the monomer with a well width  $\lambda$  of  $1.5\sigma$ , according to the Barker–Henderson perturbation theory.<sup>62</sup> For monodisperse hard-sphere chains, Banaszak et al.<sup>57</sup> have reported the increase of critical temperature as a function of chain length. We used their model to compute  $T_{\text{ph}}/T_{\text{ph}}^0$  as a function of protein volume fraction,  $\phi$ , and chain length. Here, we will focus on the monodisperse dimer. This species represents the smallest hard-sphere chain.

For the dimer, we compute  $T_{\text{ph}}/T_{\text{ph}}^0$  of 1.4 at our experimental protein concentration ( $\phi = 0.007$ ) and  $T_{\text{ph}}/T_{\text{ph}}^0$  of 1.3 around the

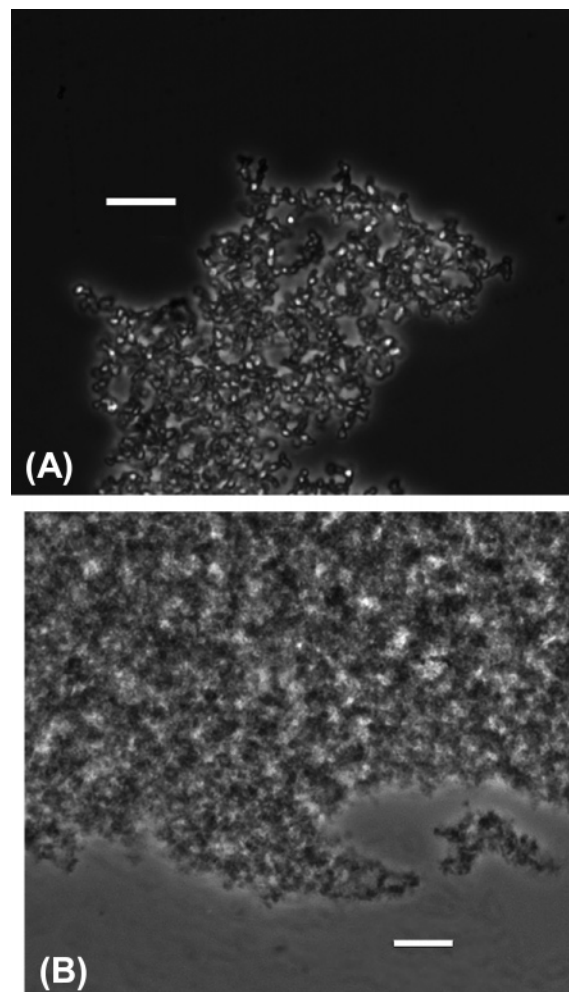


**Figure 5.** Images taken with a light microscope using phase contrast. (A) LLPS induced by lysozyme cross-linking at 25 °C. The experimental conditions are 10 mg/mL lysozyme in sodium borate buffer, 0.2 M, pH 9.0, NaCl 0.5 M,  $c_{\text{CL}} = 0.1\%$ ,  $T_{\text{ph}}^0 = -4.3$  °C. (B) Amorphous aggregation induced by lysozyme cross-linking at 25 °C. The experimental conditions are 10 mg/mL lysozyme in sodium borate buffer, 0.2 M, pH 9.0, PEG8000 2.5%,  $c_{\text{CL}} = 0.1\%$ ,  $T_{\text{ph}}^0 = -4.3$  °C. The length of the horizontal bars is 10 μm.

critical point. We can therefore conclude that all our experimental values of  $T_{\text{ph}}/T_{\text{ph}}^0$ , reported in Figure 6b are significantly lower than these theoretical predictions. The same conclusion is obtained if the Baxter potential (sticky spheres)<sup>63</sup> is employed instead of the square-well potential. A more direct, yet approximate, comparison between our experimental results and dimer prediction can be made if we consider the experimental  $T_{\text{ph}}/T_{\text{ph}}^0$  values corresponding to a number-average degree of oligomerization equal to 2. If we assume the most probable distribution,<sup>64</sup> we must consider the values of  $T_{\text{ph}}/T_{\text{ph}}^0$  at  $i_s/i_s^0$  of 4 for the comparison. We obtain  $T_{\text{ph}}/T_{\text{ph}}^0$  of 1.1 for both protein cases. This value corresponds to an increase in temperature that is only about 25% of that predicted by the model. It is, however, important to bear in mind that the accuracy of this comparison is affected by the polydisperse nature of the cross-linked protein oligomers. Fortunately, an experimental comparison of LLPS phase boundaries between monodisperse dimer and monomer has been reported using  $\gamma$ D-crystallin as a model protein.<sup>65</sup> As in our case,

(61) Reichl, L. E. *A Modern Course in Statistical Physics*; University of Texas Press: Austin, TX, 1980.

(62) Barker, J. A.; Henderson, D. *Rev. Mod. Phys.* **1976**, *48*, 587–671.

(63) Baxter, R. J. *J. Chem. Phys.* **1968**, *49*, 2770–2774.

(64) Flory, P. J. *Principles of Polymer Chemistry*; Cornell University Press: Ithaca, NY, 1953.

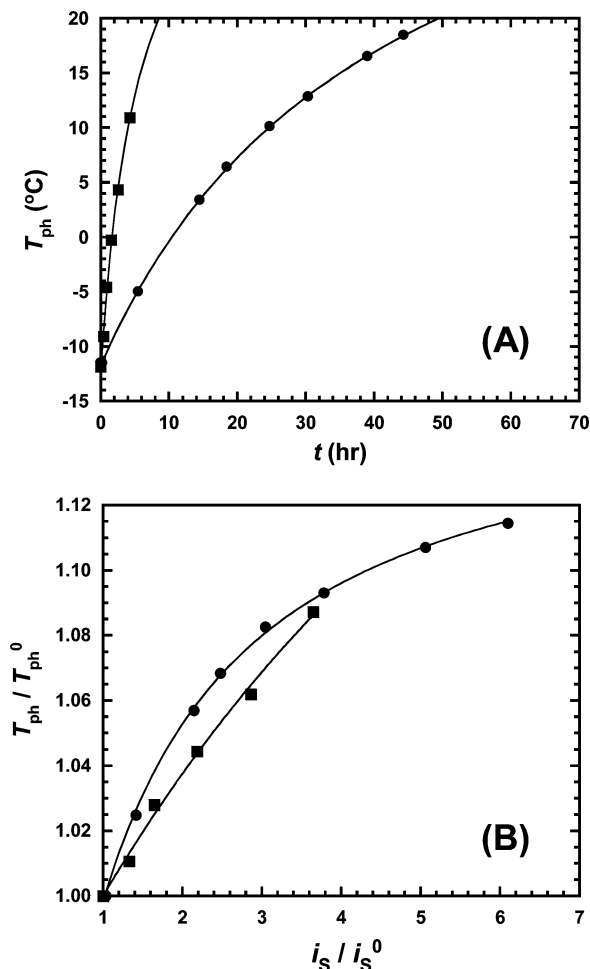


**Figure 6.** (A) LLPS temperature,  $T_{ph}$ , as a function of time,  $t$ , during cross-linking at 25 °C. These data were taken for 10 mg/mL albumin in sodium acetate buffer, 0.1 M, pH 5.2, PEG8000 6.0%,  $c_{CL} = 0.015\%$  (squares), and 10 mg/mL lysozyme in sodium acetate buffer, 0.1 M, pH 4.5, NaCl 0.5 M,  $c_{CL} = 0.050\%$  (circles). (B) Corresponding ratio of absolute temperatures,  $T_{ph}/T_{ph}^0$ , as a function of the ratio of light-scattering intensities:  $i_s/i_s^0$ . The solid curves are guides for the eye.

their experimental  $T_{ph}/T_{ph}^0$  values are also significantly lower than the theoretical prediction:  $T_{ph}/T_{ph}^0$  is 1.05 at  $\phi$  of 0.007 and 1.1 at  $\phi$  of 0.2, close to the critical point. Thus, although the model used previously qualitatively describes the increase of LLPS temperature with the degree of oligomerization, it significantly overestimates the experimental values of  $T_{ph}/T_{ph}^0$ .

**Kinetic Evolution of Oligomerization-Induced LLPS.** For both lysozyme and albumin solutions, we used DLS to examine their macromolecular size distribution as a function of time after the addition of glutaraldehyde. Figure 7 summarizes our DLS results on lysozyme at three representative glutaraldehyde concentrations. During the initial stage of cross-linking, the macromolecular distribution is monomodal. The corresponding average hydrodynamic radius,  $R_h$ , was calculated (see Materials and Methods) and reported as a function of time,  $t$ , starting from the initial hydrodynamic radius,  $R_h^0$ , of the protein monomer (circles in Figure 7). The value of  $R_h$  increases with  $t$  due to protein oligomerization. After a given induction time, there was a sharp change in total scattered intensity, and the distribution became bimodal. The second peak corresponds to protein clusters

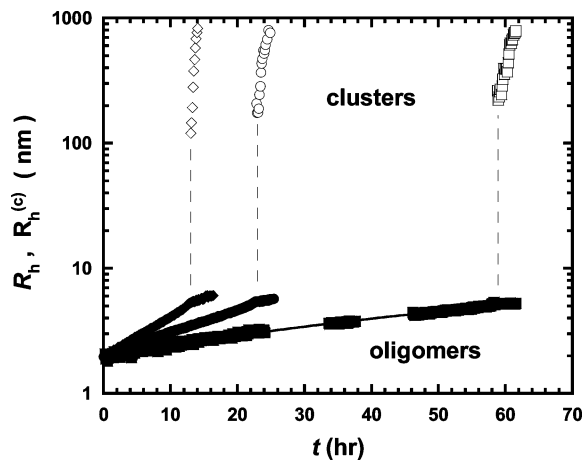


**Figure 7.** Average hydrodynamic radius of oligomers ( $R_h$ , solid data points) and mesoscopic clusters ( $R_h^{(c)}$ , open data points) as a function of time,  $t$ , during cross-linking at 25 °C and at three representative glutaraldehyde concentrations: 0.045% (squares), 0.070% (circles), and 0.090% (diamonds). The dashed vertical lines identify the light-scattering induction time for the formation of protein clusters. These data were taken for 10 mg/mL lysozyme in sodium acetate buffer, 0.1 M, pH 4.5, 0.5 M NaCl. The solid curves are guides for the eye.

with an average hydrodynamic radius,  $R_h^{(c)}$ , larger than 100 nm (squares in Figure 7). The size of these mesoscopic scattering elements increases with time. From Figure 7, we can see that the protein clusters are detected at approximately the same oligomer average radius and, consequently, at the same degree of oligomerization, independent of the cross-linker concentration.

In the case of albumin, we obtained similar results. However, the formation of protein clusters could not be quantitatively monitored by DLS due to the generally fast kinetics of phase separation. Moreover, for those cases in which the rate of phase separation was sufficiently reduced by using very low glutaraldehyde concentrations, the hydrodynamic radius of the incipient protein clusters was found to be already significantly larger than 1  $\mu\text{m}$ , which is outside the DLS domain.

Using our DLS results, we examined the effect of cross-linker concentration on both the rate of protein oligomerization and the size of the protein clusters. To examine the protein-oligomerization rate, we determined the initial slope:  $(dR_h/dt)_{t=0}/R_h^0$  as a function of glutaraldehyde concentration for both protein cases. This quantity is related to the initial oligomerization rate  $(-dc_1/dt)_{t=0}$ , where  $c_1$  is the mass concentration of the monomer. Since  $R_h$  is inversely proportional to the  $z$ -average diffusion coefficient:

$$\frac{R_h}{R_h^0} = \frac{\sum_{i=1}^{\infty} i c_i}{\sum_{i=1}^{\infty} i \alpha_i c_i} \quad (1)$$

where  $c_i$  is the mass concentration of protein species  $i$ , and  $\alpha_i$  is the ratio of the initial hydrodynamic radius to the hydrodynamic radius of species  $i$ . We have  $\alpha_1$  of 1 for the monomer by definition and  $\alpha_i < 1$  for the protein oligomers (with  $i \neq 1$ ). By differentiating eq 1 with respect to time and taking the limit of  $t \rightarrow 0$ , we obtain:

$$\frac{1}{R_h^0} \left( \frac{dR_h}{dt} \right)_{t=0} = 2(\alpha_2 - 1) \frac{1}{c_1^0} \left( \frac{dc_1}{dt} \right)_{t=0} \quad (2)$$

where  $\alpha_2 < 1$  is the ratio of  $R_h^0$  to the hydrodynamic radius of

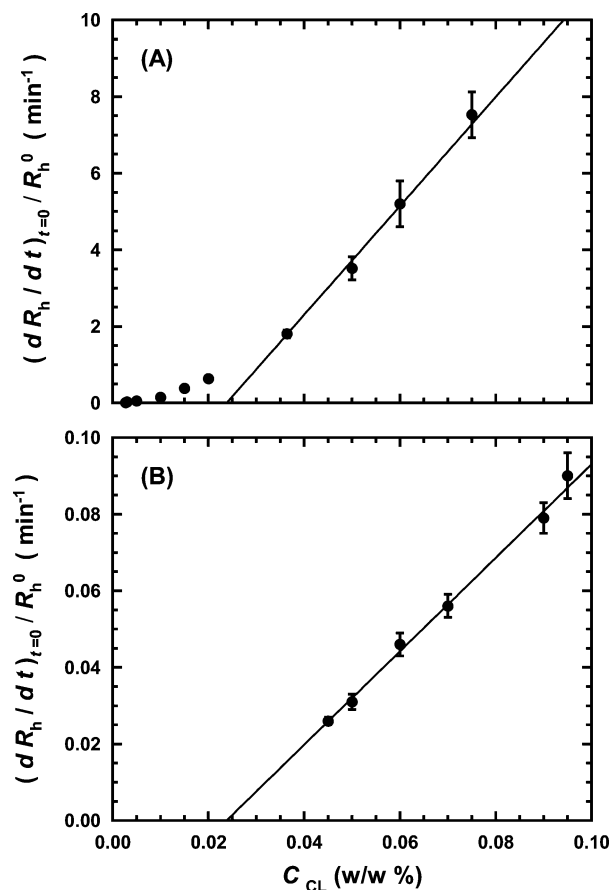


**Figure 8.** Derivative  $(dR_h/dt)_{t=0}/R_h^0$  as a function of glutaraldehyde concentration,  $c_{CL}$ , at 25 °C. (A) 10 mg/mL albumin in sodium acetate buffer, 0.1 M, pH 5.2, PEG8000 6.0% and (B) 10 mg/mL lysozyme in sodium acetate buffer, 0.1 M, pH 4.5, 0.5 M NaCl. The data with  $c_{CL} > 0.025\%$  were fit to straight lines.

the dimer, and  $c_1^0$  is the monomer mass concentration at  $t = 0$  (i.e., the total mass concentration). We therefore conclude that  $(dR_h/dt)_{t=0}/R_h^0$  is directly proportional to  $(-dc_1/dt)_{t=0}$ .

In Figure 8a,b, we report  $(dR_h/dt)_{t=0}/R_h^0$  as a function of the glutaraldehyde concentration,  $c_{CL}$ , for both albumin (Figure 8a) and lysozyme (Figure 8b). As expected, we observed that the oligomerization rate for albumin is significantly higher than that for lysozyme at all experimental glutaraldehyde concentrations. The increase in reaction rate with glutaraldehyde concentration shows a significant deviation from linearity in both cases, and the reaction order with respect to glutaraldehyde was found to be  $1.90 \pm 0.05$  for albumin and  $1.6 \pm 0.1$  for lysozyme. We further observe that, for glutaraldehyde concentrations higher than  $c_{CL}^0 \approx 0.025\%$  (w/w), the oligomerization rate can be regarded as directly proportional to  $(c_{CL} - c_{CL}^0)$  for both protein cases (see Figure 8a,b). Since the concentration of glutaraldehyde oligomers increases with  $c_{CL}$ , our results are consistent with a reaction mechanism in which the presence of glutaraldehyde oligomers is necessary for protein cross-linking.

We now examine the dependence of the hydrodynamic radius,  $R_h^{(c)}$ , of the incipient protein clusters on cross-linker concentration. Since the values of  $R_h^{(c)}$  are closely related to the corresponding critical radii for the nucleation of the protein-rich droplets, they can be used to examine the effect of cross-linker concentration on nucleation. In Figure 9a, we report  $R_h^{(c)}$  at the light-scattering induction time (vertical dashed lines in Figure 7) as a function of glutaraldehyde concentration,  $c_{CL}$ , for lysozyme.

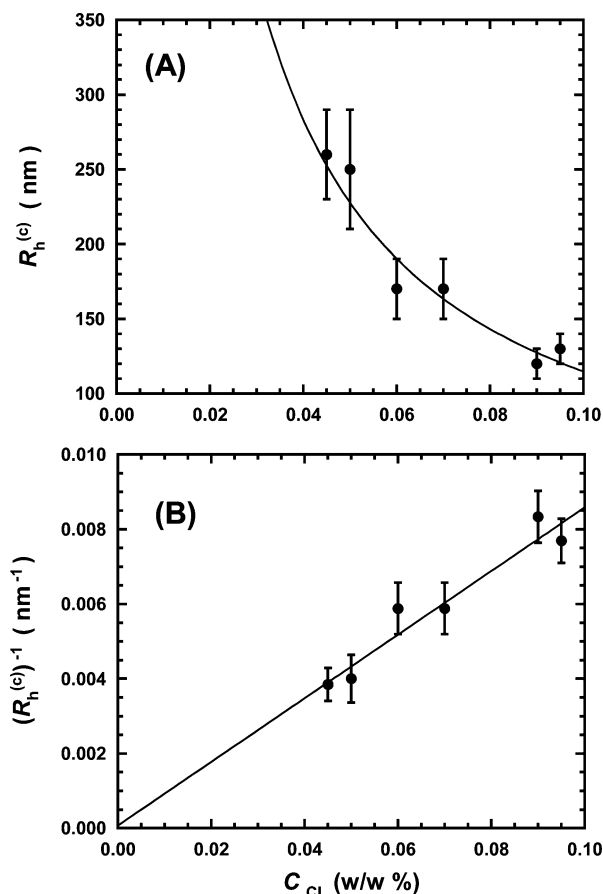


**Figure 9.** (A) Average hydrodynamic radius,  $R_h^{(c)}$ , as a function of glutaraldehyde concentration,  $c_{CL}$ . The experimental conditions are those described in Figure 7. (B) Inverse of  $R_h^{(c)}$  as a function of  $c_{CL}$ . The  $(R_h^{(c)})^{-1}$  data were fitted to straight lines.

We can see that  $R_h^{(c)}$  decreases as  $c_{CL}$  increases. Correspondingly,  $(R_h^{(c)})^{-1}$  linearly increases with  $c_{CL}$  in Figure 8b. Our results imply that the final supersaturation with respect to nucleation increases with cross-linker concentration. This behavior, which is analogous to that shown for the radius of albumin microspheres in Figure 2a,b, corroborates the hypothesis that the final size of albumin microspheres is controlled by nucleation, whereas that of lysozyme microspheres is significantly affected by the droplet growth rate.

## Conclusion

We demonstrated that the formation of protein-rich droplets can be isothermally induced by protein cross-linking in aqueous solutions. These droplets evolve into cross-linked protein microspheres. We related this phenomenon to the LLPS properties of the protein monomer and to the increase of LLPS temperature during protein oligomerization. When macroscopic aggregation competes with LLPS, a rationale choice of pH, PEG, and salt concentrations may be used to favor LLPS relative to aggregation. This work contributes to the fundamental understanding on both phase transitions of protein solutions and morphology of cross-linked protein precipitates. It also provides guidance for the development of new methods for the stabilization of the protein liquid cluster and the preparation of protein-based materials. The mild conditions of temperature and chemical environment used in these experiments also can be extended to more labile proteins.

**Acknowledgment.** We acknowledge Aleksey Lomakin and Igor Yudin for valuable discussions on the dynamic light-scattering technique and John Albright for valuable comments concerning the manuscript. This work was supported by the ACS

Petroleum Research Fund (47244-G4) and TCU Research and Creative Activity Funds.

LA703223F